

# Phase Transition of DNA-Linked Gold Nanoparticles

Ching-Hwa Kiang

*Department of Physics & Astronomy, Rice University, Houston, TX 77005*

---

## Abstract

Melting and hybridization of DNA-capped gold nanoparticle networks are investigated with optical absorption spectroscopy. Single-stranded, 12-base DNA-capped gold nanoparticles are linked with complementary, single-stranded, 24-base linker DNA to form particle networks. Compared to free DNA, a sharp melting transition is seen in these networked DNA-nanoparticle systems. The sharpness is explained by percolation transition phenomena.

---

## 1 Introduction

DNA melting and hybridization phenomena are of great importance in both fundamental biological science and biotechnology [1–4]. Sequence-specific DNA recognition is important in detection, diagnosis of genetic diseases, and identification of infectious agents. DNA-gold nanoparticle systems undergo a change of color upon network formation, which can be used for highly sensitive detection when specific nucleic acid sequences induce network formation [5]. Indeed, such a system has been demonstrated to be useful to detect anthrax and other agents of biowarfare [6].

Here we report studies of DNA-gold nanoparticle melting transitions. DNA-gold nanoparticles were prepared using modified methods based on Ref. [5]. The basic unit is illustrated in Fig. 1. Gold nanoparticles are derivatized with non-complementary, single-stranded, 12-base DNA ( $\sim 4$  nm). Upon adding 24-base, complementary linker DNA, particles aggregate to form network structures, and precipitate out of the solution.

DNA-functionalized gold nanoparticles were prepared by conjugating gold nanoparticles ranging from 10 to 40 nm in diameter (Sigma, ICN Pharmaceutical) with thiol-modified DNA [5,7]. 3'-alkanethiol DNA 3'S-(CH<sub>2</sub>)<sub>3</sub>-ATG-CTC-AAC-TCT was prepared by using C3 S-S modifier and 5'-alkanethiol

DNA TAG-GAC-TTA-CGC-(CH<sub>2</sub>)<sub>6</sub>-S5' by C6 S-S on a 1  $\mu$ mol scale and purified by HPLC (Invitrogen). Just prior to conjugation with gold, 100 nmol of the dried DNA was redispersed in 400  $\mu$ l of 0.1 M DTT, 0.1 M phosphate buffer (pH 8) solution at room temperature for 30 minutes to cleave the disulfide bond. Salt was removed with a NAP-5 desalting column to avoid bare gold aggregation prior to DNA conjugation.

The deprotected alkanethiol-modified DNA were used to derivatize gold nanoparticles at room temperature for 24 hours to form gold nanoparticle probes. The solutions were then brought to 0.3 M NaCl, 10 mM phosphate buffer (pH 7) and allowed to stand for 48 hours. To remove excess DNA, solutions were centrifuged at 13,200 *rpm* (16,110 $\times$ *G*) for 60 minutes. The supernatant was decanted, and the red precipitate was redispersed in 1 ml nanopure water and centrifuged again. After decanting the supernatant, about 200  $\mu$ l of precipitate of each modified gold nanoparticles were collected for spectroscopic investigation.

20 nmol linker DNA 3'GCG-TAA-GTC-CTA-AGA-CTT-GAG-CAT5' (Invitrogen) was dispersed in 1 ml solution of 0.3 M NaCl, 10 mM phosphate buffer (pH 7). Hybridization of linkers with gold nanoparticles was done by mixing 200  $\mu$ l each modified gold nanoparticles (0.8 OD) with 8  $\mu$ l linker solution (10 pmol/ $\mu$ l). The solution was annealed at 70  $^{\circ}$ C for 10 minutes and cooled to room temperature during a 2 hour period and was allowed to aggregate for several days.

Absorption spectra of DNA-modified gold nanoparticles were taken on a Hewlett-Packard diode array spectrophotometer (HP8453). The kinetics of formation of network nanoparticle structures at room temperature is illustrated in Fig. 2. Upon adding linker DNA, gold nanoparticles aggregate to form networks, as demonstrated in the gold surface plasmon peak (520 nm) shift of the DNA-modified gold nanoparticles [8,9]. The aggregation started with the wavelength shift of the plasmon band, followed by broadening and more shifting of the peak as hybridization continues. From molecular simulations it is known that change in network size results mainly in peak broadening, whereas change in gold volume fraction results mainly in peak shifting [10]. Our results indicate that the initial aggregation has characteristics consistent with increasing volume fraction, followed by increasing network size.

To study the equilibrium behavior of DNA-gold nanoparticle system, we monitor the UV-visible spectra absorption intensity at 260 nm and 520 nm while melting the DNA-gold nanoparticle network. DNA bases have strong absorption at the UV region, and the peak near 260 nm is a result of combination of these electronic transition dipoles [11]. The DNA double helix has smaller extinction coefficient than single-stranded DNA due to hypochromism and, therefore, the absorption intensity at 260 nm increases as a result of DNA melting.

The sample was heated by a peltier temperature controller (JASCO J-715) at a rate of 0.5 °C/min, from 25 to 75 °C. The 260 nm and 520 nm melting curves are very similar, indicating that DNA and nanoparticle melting are closely related. Figure 3a displays the melting curves of 10 nm, 20 nm, and 40 nm gold particles with linker DNA. The melting transition width (FWHM) is about 5°C, compared to 12°C for melting of free DNA [12]. As illustrated in the figure, the transition width as well as the melting temperature  $T_m$  of DNA have been dramatically modified by the binding to gold particles.

Figure 3b illustrates two different transitions at high  $T$  and low  $T$ . The absorption of DNA-modified, 10 nm, 20 nm, and 40 nm gold nanoparticles are plotted versus reduced temperatures ( $T_R = T/T_m$ ). Above temperature  $T_m$  (low connectivity), the curves appear insensitive to details, indicative of universal scaling at the percolation transition [13]. The curves can be fitted with an equation that describes percolation phenomena,

$$A(T_R) = 1 - a(T_c - T_R)^\beta$$

where  $A(T_R)$  is the absorption as a function of reduced temperature  $T_R$ , and  $\beta$  is the critical exponent for percolation. In three-dimensions,  $\beta = 0.403$  [14]. The parameters  $a$  and  $T_c$  are adjustable. Using the data for all three particle sizes for  $1 < T_R < 1.003$ , we obtained  $a=4.079$  and  $T_c=1.005$ , as shown in Fig. 3b. The deviation from the fit above  $T_c$  is presumably due to finite size effects [15].

The growth mechanism of the DNA-gold nanoparticle network is illustrated in Figure 4. Particles initially are dissolved in the solution. With the addition of complementary linker DNA, hybridization occurs, and the particles form a network-like structure. The volume fraction of the porous structure continues to increase past the percolation threshold, and eventually the clusters become a dense amorphous structure.

In conclusion, the network formation in DNA-gold particle systems exhibits a phase transition, which does not occur for short DNA. Our results provide detailed and precise measurements of hybridization/melting of the DNA-gold nanoparticle system. DNA attached to gold is a controlled system in which to do experiments on phase transitions and serves as a good probe for many biological systems that involve DNA. This is a new system, about which relatively little is known. Many parameters, such as the length of DNA, particle size, degree of disorder, solution pH value, and salt concentration, may be varied to better understand the system.

\*To whom correspondence should be addressed, Email: [chkang@rice.edu](mailto:chkang@rice.edu).

## References

- [1] R. M. Wartell and A. S. Benight, Phys. Rep. **126**, 67 (1985).
- [2] D. Cule and T. Hwa, Phys. Rev. Lett. **79**, 2375 (1997).
- [3] C. A. Gelfand *et al.*, Proc. Natl. Acad. Sci. USA **96**, 6113 (1999).
- [4] N. L. Goddard, G. Bonnet, O. Krichevsky, and A. Libchaber, Phys. Rev. Lett. **85**, 2400 (2000).
- [5] J. J. Storhoff *et al.*, J. Am. Chem. Soc. **120**, 1959 (1998).
- [6] C. A. Mirkin, Inorg. Chem. **39**, 2258 (2000).
- [7] L. A. Chrisey, G. U. Lee, and C. E. O’Ferrall, Nucleic Acids Res. **24**, 3031 (1996).
- [8] A. A. Lazarides and G. C. Schatz, J. Phys. Chem. B **104**, 460 (2000).
- [9] S. Link and M. A. El-Sayed, J. Phys. Chem. **103**, 8410 (1999).
- [10] J. J. Storhoff *et al.*, J. Am. Chem. Soc. **122**, 4640 (2000).
- [11] *Biophysical Chemistry, Part II: Techniques for the study of biological structure and function*, edited by C. R. Cantor and P. R. Schimmel (W. H. Freeman and Company, New York, 1980).
- [12] R. Elghanian *et al.*, Science **277**, 1078 (1997).
- [13] J. Rudnick, P. Nakmahachalasint, and G. Gaspari, Phys. Rev. E **58**, 5596 (1998).
- [14] R. J. Creswick, H. A. Farach, and C. P. Poole, Jr., in *Introduction to Renormalization Group Methods in Physics* (John Wiley & Sons, New York, 1992), pp. 69–107.
- [15] M. W. Deem and J. M. Newsam, J. Phys. Chem. **99**, 14903 (1995).
- [16] J. Rudnick and R. Bruinsma, Biophys. J. **76**, 1725 (1999).

Fig. 1. Basic building block of gold nanoparticles capped with 12-base DNA with thiol-modification at 3'( $D1$ ) or 5'( $D2$ ) end.  $L$  is linker DNA composed of 24-base DNA complementary to the capping DNA  $D1$  and  $D2$ . Capping DNA is bound to gold nanoparticles through covalent bonds, and the linker DNA  $L$  binds the capping DNA through hydrogen bonds.

Fig. 2. Optical absorption spectra of DNA-modified gold nanoparticles. The time starts when linker  $L$  is added to the solution containing mixtures of gold nanoparticles modified with  $D1$  and  $D2$ . Owing to the particle network formation, the 520 nm gold surface plasmon peak slowly shifts to longer wavelength, followed by peak broadening and further shifting.

Fig. 3. Normalized melting curves of linked gold nanoparticle networks monitored at 260 nm. (a) Melting curves of different size particles as a function of temperature. Inset shows the change in melting temperature,  $T_m$ , with particle diameter  $D$ . The line is a fit to a power law. (b) Melting of particles as a function of reduced temperature. Solid line shows the region where data were used for curve fitting, dashed line is calculated from the equation of best fit (see text). The scaling shows the universality of the melting transition above the transition temperatures.

Fig. 4. Growth mechanism of the DNA-gold nanoparticle network. When linker DNA is added, hybridization occurs, connecting the gold nanoparticle into porous networks. As the cluster grows, the volume fraction and the size of the cluster continue to increase. The transition between dispersed nanoparticles and micrometer sized cluster appears to be a cooperative phenomenon [16], much like a phase transition.

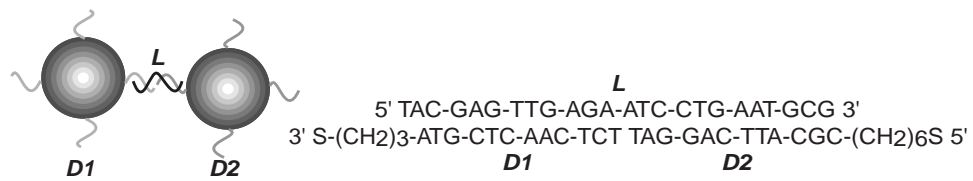


Figure 1. Kiang, "Phase Transition . . ."

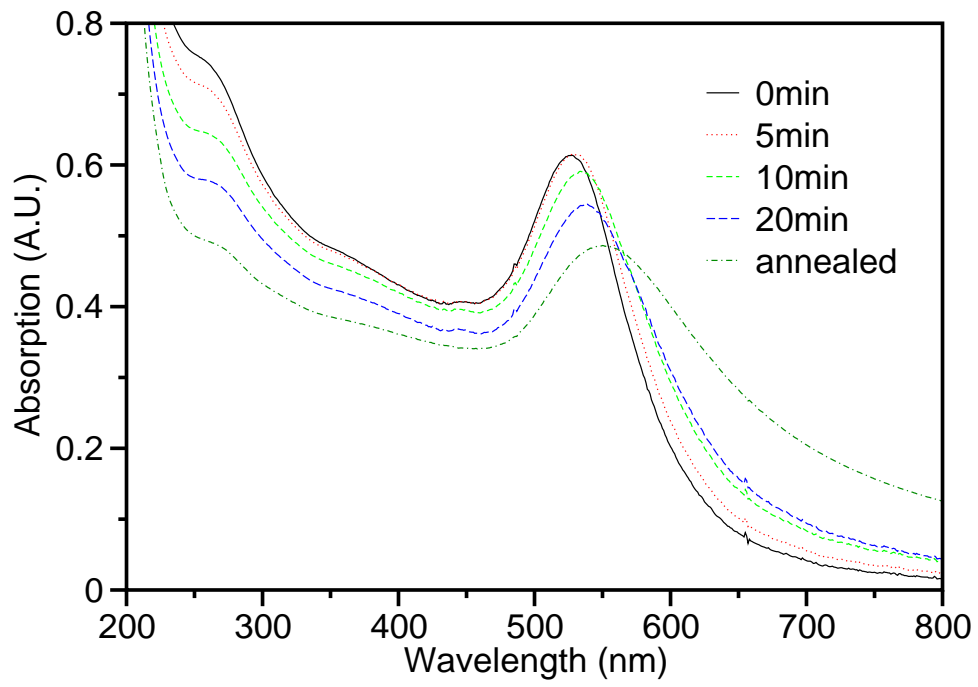


Figure 2. Kiang, "Phase Transition ..."

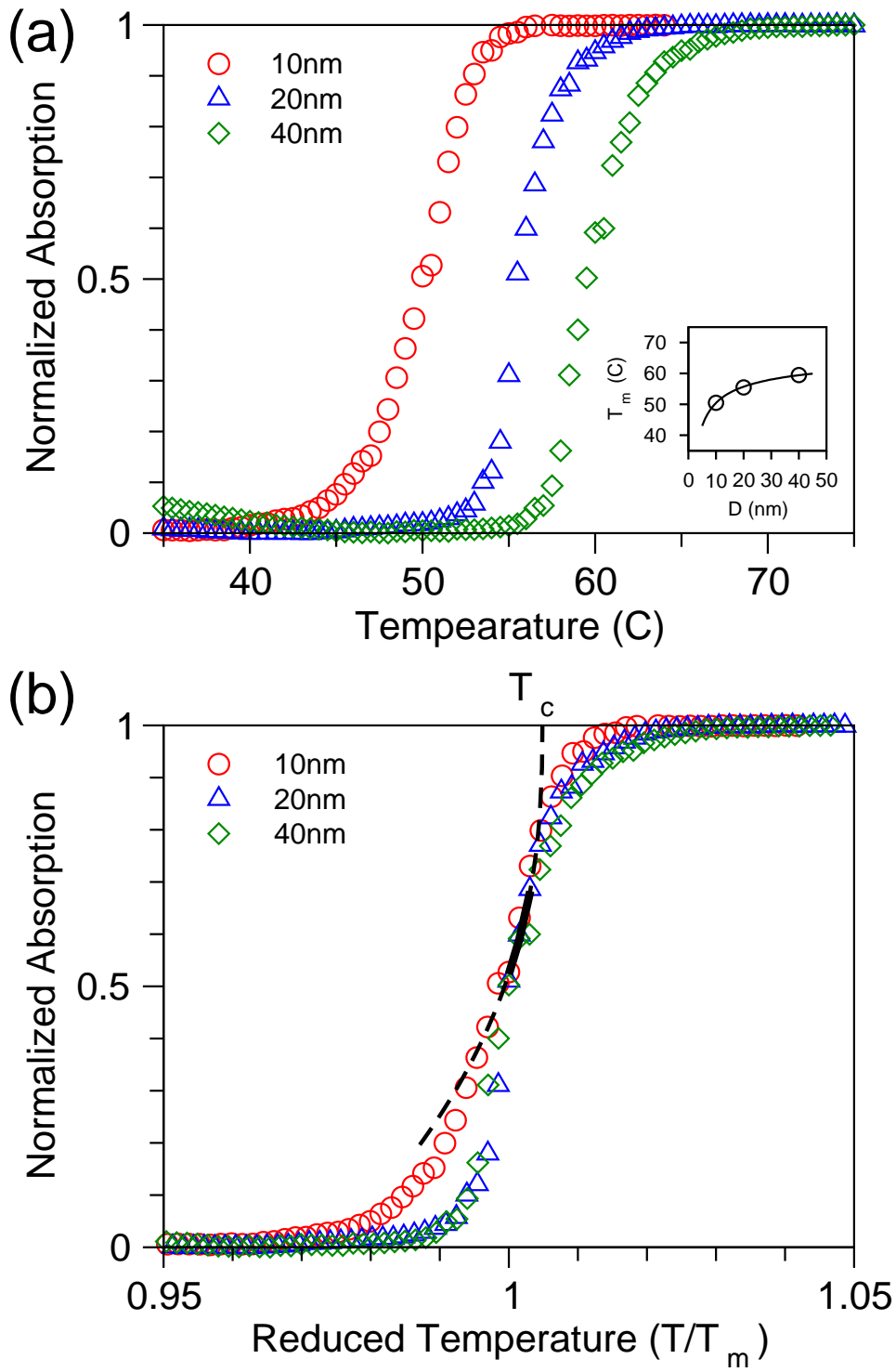


Figure 3. Kiang, "Phase Transition . . ."



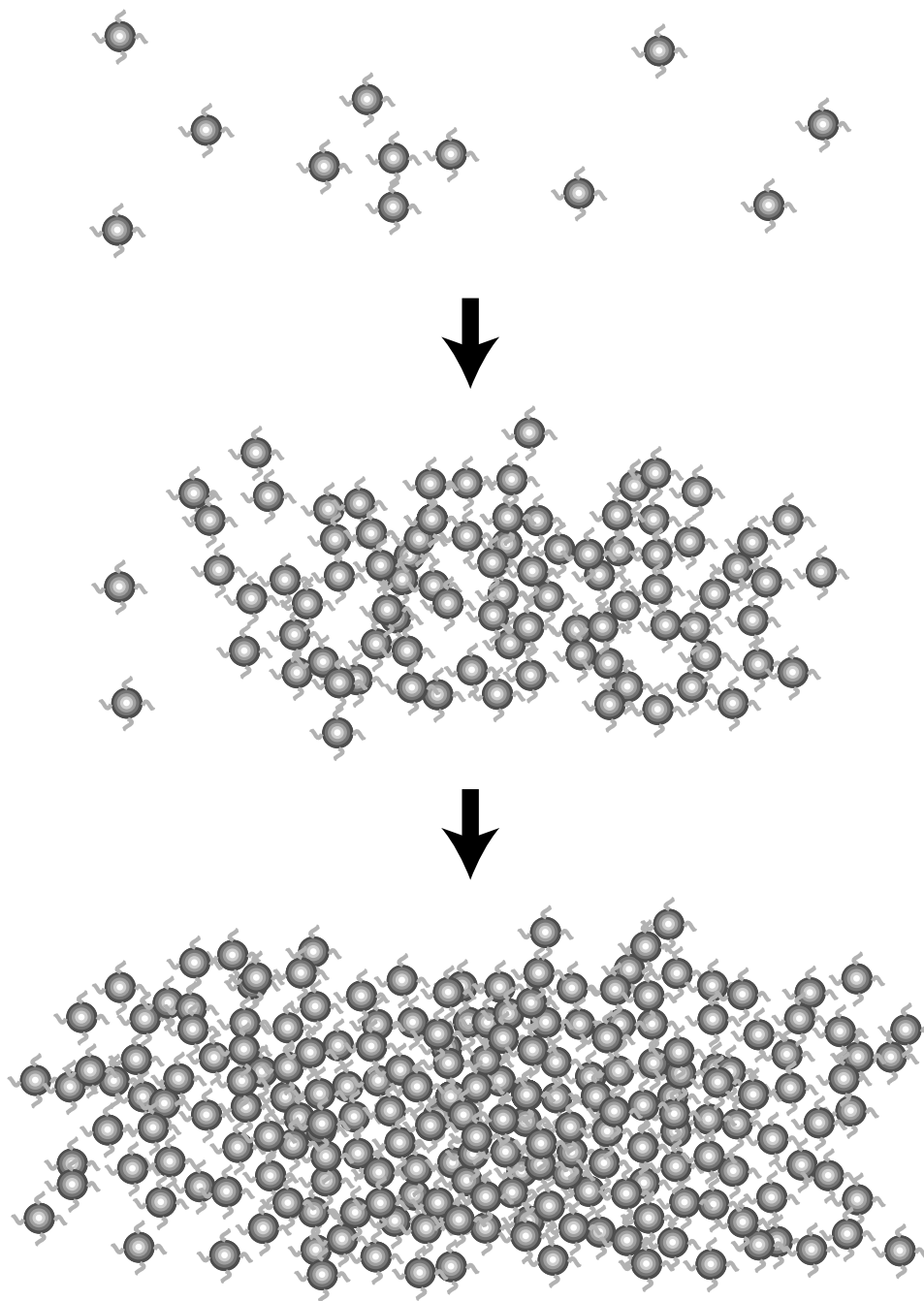


Figure 4. Kiang, “Phase Transition . . . .”